Modulation of Epstein-Barr Virus Glycoprotein B (gB) Fusion Activity by the gB Cytoplasmic Tail Domain

Nicholas J. Garcia, Jia Chen, Richard Longnecker

Department of Microbiology and Immunology, The Feinberg School of Medicine, Northwestern University, Chicago, Illinois, USA

ABSTRACT **Epstein-Barr virus (EBV), along with other members of the herpesvirus family, requires a set of viral glycoproteins to mediate host cell attachment and entry. Viral glycoprotein B (gB), a highly conserved glycoprotein within the herpesvirus family, is thought to be the viral fusogen based on structural comparison of EBV gB and herpes simplex virus (HSV) gB with the postfusion crystal structure of vesicular stomatitis virus fusion protein glycoprotein G (VSV-G). In addition, mutational studies indicate that gB plays an important role in fusion function. In the current study, we constructed a comprehensive library of mutants with truncations of the C-terminal cytoplasmic tail domain (CTD) of EBV gB. Our studies indicate that the gB CTD is important in the cellular localization, expression, and fusion function of EBV gB. However, in line with observations from other studies, we conclude that the degree of cell surface expression of gB is not directly proportional to observed fusion phenotypes. Rather, we conclude that other biochemical or biophysical properties of EBV gB must be altered to explain the different fusion phenotypes observed.**

IMPORTANCE **Epstein-Barr virus (EBV), like all enveloped viruses, fuses the virion envelope to a cellular membrane to allow release of the capsid, resulting in virus infection. To further characterize the function of EBV glycoprotein B (gB) in fusion, a comprehensive library of mutants with truncations in the gB C-terminal cytoplasmic tail domain (CTD) were made. These studies indicate that the CTD of gB is important for the cellular expression and localization of gB, as well as for the function of gB in fusion. These studies will lead to a better understanding of the mechanism of EBV-induced membrane fusion and herpesvirus-induced membrane fusion in general, which will ultimately lead to focused therapies guided at preventing viral entry into host cells.**

Received 4 December 2012 **Accepted** 10 December 2012 **Published** 22 January 2013

Citation Garcia NJ, Chen J, Longnecker R. 2013. Modulation of Epstein-Barr virus glycoprotein B (gB) fusion activity by the gB cytoplasmic tail domain. mBio 4(1):e00571-12. doi:10.1128/mBio.00571-12

Editor Michael Imperiale, University of Michigan

Address correspondence to Richard Longnecker, r-longnecker@northwestern.edu.

Epstein-Barr virus (EBV) is a member of the *Gammaherpesviridae* subfamily of herpesviruses, which has a pronounced prevalence in humans, as up to more than 90% of the world's population is estimated to be latently infected with EBV (1). Primary EBV infection can result in infectious mononucleosis in adolescence yet is generally asymptomatic in childhood primary infections (1). Virions acquired in saliva must be deposited into the epithelial cells lining the oral pharynx for transmission to occur (1). Infection through sexual intercourse, organ transplantation, and blood transfusion are also routes of transmission (1). After the initial transmission of the virus into the host, EBV infects B cells and remains in a largely latent state in memory B cells, evading the host immune response and thereby allowing long-term persistence in the host (2, 3). Reactivation occurs periodically throughout the life of the host, generating virus to infect naive hosts (1). EBV has been linked to the development of several cancers, including Burkitt's lymphoma, Hodgkin's lymphoma, T cell lymphomas, and epithelial malignancies, such as gastric carcinoma and nasopharyngeal carcinoma (1).

As described above, EBV infects epithelial and B cells in the host, with fusion of the virus envelope with cell membranes of the host cell being a requisite step in the entry process, as with other herpesviruses (4, 5). This process requires the cooperative function of multiple viral glycoproteins (4, 5). For B cells, glycoprotein 42 (gp42), the glycoprotein complex gH/gL, and glycoprotein B (gB) are essential for EBV glycoprotein-mediated fusion, whereas with epithelial cells, only gB and the gH/gL complex are essential for EBV glycoprotein-mediated fusion (5). The roles of these individual glycoproteins in regulating fusion are subject to investigation, but of particular interest in this study is gB.

EBV gB is an 857-amino-acid protein with a long amino-terminal ectodomain that includes nine potential N-linked glycosylation sites and a predicted 22-amino-acid cleavable signal sequence at the N terminus (6). Based on our studies (7) and comparison with herpes simplex virus 1 (HSV-1) gB (8), we conclude that the most C-terminal of three hydrophobic domains found in the primary amino acid sequence of EBV gB (6, 9) is the transmembrane domain (TM), which is required for membrane anchoring. Following the TM, there is a 104-amino-acid C-terminal cytoplasmic tail (6), which is the main subject of this paper and herein referred to as the cytoplasmic tail domain (CTD).

Of the variety of glycoproteins encoded by the herpesvirus family genomes, gB is one of the most conserved glycoproteins,

with homologues in each of the subfamilies (9, 10). The recent resolution of the crystal structures of EBV gB (11) and HSV-1 gB (12) and their structural resemblance to the postfusion structure of the vesicular stomatitis virus fusion protein glycoprotein G (VSV-G), for which both pre- and postfusion structures have been solved (13, 14), implicate gB as the herpesvirus fusogen. In the crystal structure of VSV-G, internal fusion loops comprising the putative fusion motif were identified (13), and comparable fusion loops appear to be structurally conserved in the crystal structures of HSV-1 gB (12) and EBV gB (11). Mutagenic studies of the putative fusion loops in HSV-1 gB (15, 16) and EBV gB (7, 17) perturb fusion, further indicating the fusogen role of gB.

Early immunofluorescence studies examining the expression of EBV gB in EBV-infected lymphocytes and transfected epithelial cells found that gB was expressed abundantly in the perinuclear region of cells and in the cytoplasm, with little-to-no detection of gB expression in the plasma membrane (9, 18). Immunoelectron microscopy of induced infected lymphocytes further demonstrated that EBV gB localized to the inner and outer nuclear membranes and also in some cytoplasmic vesicles, with little-to-no gB in the plasma membrane or in enveloped virus (9, 18).

Interestingly, one of our studies revealed that two deletion mutations in the EBV gB CTD resulted in abundant expression of gB in the plasma membrane, in contrast to the observed wild-type (WT) expression patterns noted above (19). It was postulated that this observed localization phenotype was due to the deletion of four consecutive arginine (R) residues (RRRR amino acids 836 to 839) positioned near the C terminus of the CTD (19), which was further explored by the construction of mutants in which nonendogenous residues (lysine [K], glutamic acid [E], threonine [T]) were substituted for the arginine residues in the domain, designated gB RKRR, gB KKKK, gB REER, and gB RTTR (20). The observed phenotypes suggested not only that the positive charge of the domain is important for EBV gB subcellular localization to the endoplasmic reticulum/perinuclear network but also that the structural conformation of the residues in the arginine repeat domain are of importance (20).

In order to determine if these arginine repeat domain substitution mutations which altered the localization of EBV gB could in turn affect the function of EBV gB in fusion, the mutants were tested in a virus-free cell fusion assay along with previously generated EBV gB truncation mutants, namely, gB841S, gB816, and gB801, which have progressively truncated CTDs (19, 21) (Fig. 1C, arrows). It was found that gB841S and the arginine repeat domain substitution mutant gB RKRR had little cell surface expression, like WT EBV gB, but that truncation mutants gB801 and gB816 and substitution mutants gB KKKK, gB RTTR, and gB REER had pronounced cell surface expression severalfold greater than that of WT gB (19–21). When tested in fusion with B cell targets, it was observed that gB841S and gB RKRR coexpressed with gH/gL and gp42 had fusion levels comparable to that observed for WT gB coexpressed with gH/gL and gp42 (21). Mutant gB816, which has a shorter CTD than gB841S, had a hyperfusogenic phenotype, yet gB801, which has a shorter CTD than gB816, led to a shift to low levels of fusion, significantly below levels detected for WT gB (21). In spite of the increased levels of cell surface expression for the gB KKKK, gB RTTR, and gB REER mutants, these mutants reflected fusion levels that paralleled that of WT gB (21). This suggested that the altered expression of these gB mutants from that of the WT profile could not alone explain the hyperfusogenic and hypofusogenic phenotypes and that the residues in the EBV gB CTD bounded by these truncations may play a role in regulating EBV fusion activity (21). The truncation mutants and substitution mutants used in this study were further examined in their fusion with epithelial cell targets (22). Mutant gB816, when coexpressed with gH/gL, was hyperfusogenic analogously to gB816 in fusion with B cell targets (21, 22). However, mutants gB841S and gB801 displayed phenotypes in epithelial cell fusion different from their phenotypes when coexpressed with gp42 and gH/gL in B cell fusion experiments. Notably, gB841S substantially reduced fusion with epithelial targets compared to the fusion observed with WT gB. Mutant gB801, which normally has a fusion-null phenotype in B cell target fusion experiments (21), mediated fusion with epithelial targets at notable levels yet at diminished levels compared to those of WT gB (22).

Collectively, these data from early studies with EBV gB and the EBV gB CTD suggest an important role for the CTD not only in regulating gB expression but also in regulating fusion activity in both EBV host cell types. However, these studies utilized a limited panel of mutants. In the current study, we sought to comprehensively examine the function of the gB CTD by constructing an extensive panel of truncation mutants and testing these mutants for expression and cellular localization, as well as for fusion function with B cell and epithelial cell targets.

RESULTS

Generation of truncation mutants within the EBV gB CTD. A total of 20 truncation mutations spanning the EBV gB CTD were constructed by adding a stop codon by site-specific mutation within the CTD of the gB open reading frame. Primary amino acid sequences of the gB CTD mutant library are shown, along with the previously constructed gB841S, gB816, gB801, and gB798 mutants (19, 23) (Fig. 1C, arrows). Mutant gB841S ends with amino acid 841 of gB and has the addition of 2 amino acids that differ from the amino acids found endogenously in gB. Similarly, gB816 ends at amino acid 816 of gB and has three additional nonendogenous amino acids inserted in frame before the stop codon. Construct gB801 actually ends at amino acid 800 of gB. CTD mutants constructed for this study were named based on the full amino acid length of the construct. For example, gB757 contains amino acids 1 to 757 of gB (Fig. 1C).

The comprehensive library of CTD truncation mutants span from the TM-proximal region of the CTD to the C-terminus-proximal region of the CTD. We chose to focus constructs in several regions of interest in the CTD, including near the arginine repeat domain (amino acids 836 to 839) (lowercase "rrrr" in Fig. 1C) previously shown to be important for the intracellular localization of gB, as well near a number of putative endocytosis motifs, including YPGI (amino acids 768 to 771), YHDP (amino acids 840 to 843), and LL (amino acids 849 to 850) (boldface in Fig. 1C). Furthermore, constructs were made adjacent to gB801, gB816, and gB841S mutants in order to further fine map functional domains of the gB CTD. The mutants were sequenced to confirm the presence of the desired truncation mutation in the CTD. A secondary-structure prediction of the CTD (24, 25) is included in Fig. 1B. A summary of observed fusion and cell surface expression phenotypes is included in Fig. 1C and described in greater detail below.

Cellular expression of EBV gB CTD mutants. The gB CTD truncation mutants were transfected into CHO-K1 cells and ana-

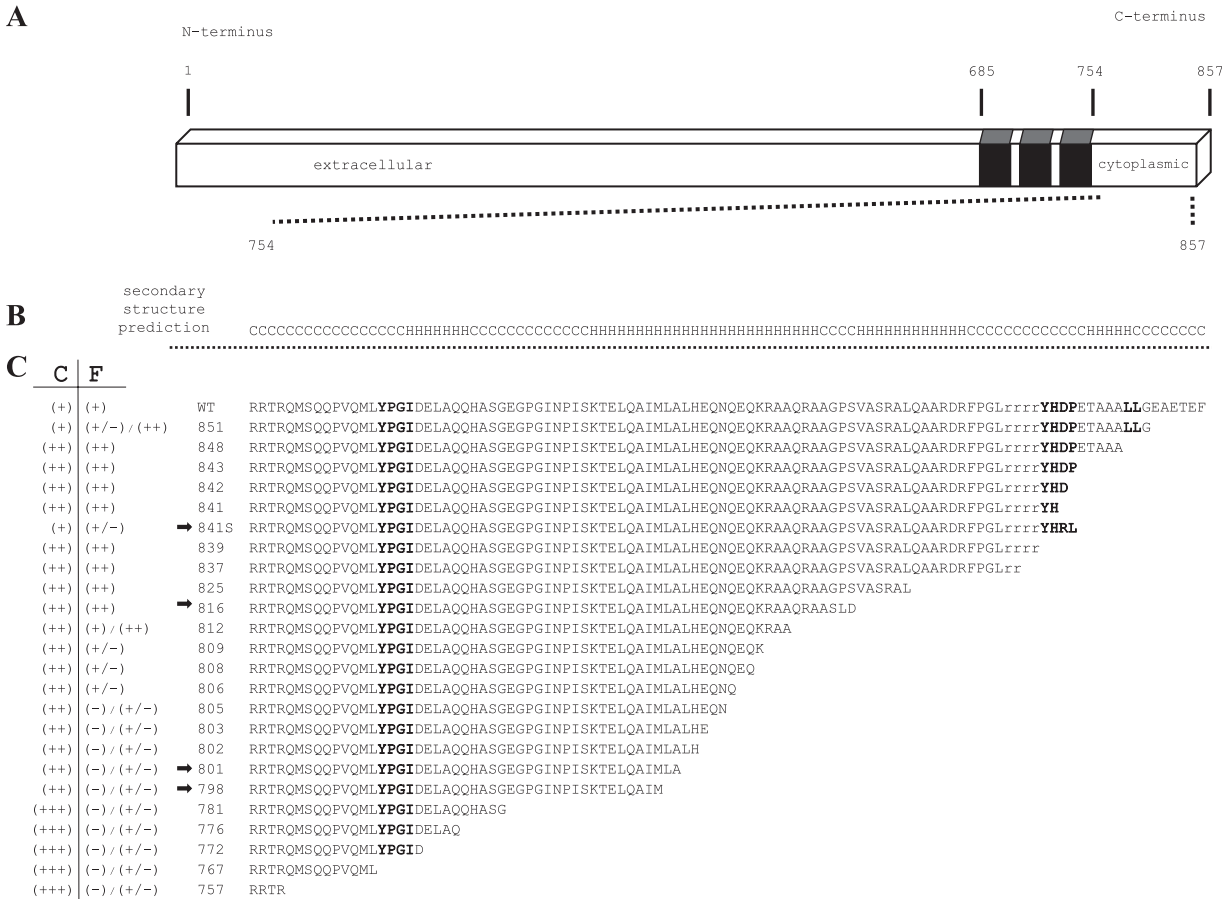

FIG 1 Schematic representation of EBV gB and the EBV gB CTD constructs. (A) Diagram of EBV gB, highlighting the long N-terminal extracellular domain, the three hydrophobic domains, with the last domain serving as the transmembrane domain (black boxes), and the 104-amino-acid CTD; (B) secondary structure prediction (generated by PSIPRED3.0 [24, 25]) for the EBV gB CTD, where "C" indicates "coil" and "H" indicates "helix"; (C) primary amino acid sequence of the WT EBV gB CTD compared to the primary amino acid sequences of previously generated EBV gB CTD mutants (indicated by arrows at the left of mutant numeric designations) and mutants generated for this study. Primary amino acid sequences are abbreviated using the single-letter amino acid abbreviations. The numeric demarcations of CTD mutants generated for this study represent the numbers of amino acids in the full-length construct. Note that previously generated gB841S has two additional nonendogenous amino acids added at the end, gB816 has three additional nonendogenous amino acids added at the end, and gB801 is actually 800 amino acids. The arginine repeat domain (amino acids 836 to 839) is shown in lowercase lettering (rrrr). Putative endogenous endocytosis motifs YPGI (amino acids 768 to 771), YHDP (amino acids 840 to 843), and LL (amino acids 849 to 850) are shown in bold lettering, along with nonendogenous YHRL (amino acids 840 to 843 of gB841S), manifested as a result of the two additional nonendogenous amino acids (arginine and leucine) added at the end of gB841S as a result of previous cloning manipulations. "C" and "F" column headings separate and summarize observed cELISA and fusion phenotypes, respectively. Under the "C" cELISA column, (+) represents WT gB-like cell surface expression (which is not expressed well at the cell surface), (++) represents intermediate levels of surface expression (greater than that of WT gB), and (+++) represents very high levels of surface expression. Under the "F" cell fusion column, (−) represents the fusion-null phenotype (at or below background levels of fusion), (+/−) represents hypofusion (fusion levels above background but below 90% of the level observed for WT gB), (+) represents WT gB-like levels of cell fusion (90% to 110% of the fusion level observed for WT gB), and (++) represents hyperfusion (fusion levels over 110% of that observed for WT gB). If there are differences in fusion observed between B cell-associated fusion and epithelial cell-associated fusion, this is indicated with a slash separating the B cell-associated fusion phenotype from the epithelial cell-associated fusion phenotype, respectively.

lyzed by cell enzyme-linked immunosorbent assay (cELISA) to examine cell surface expression (Fig. 2A and B) and by Western blotting to analyze total cellular gB expression (Fig. 2C). The cELISAs were performed in conjunction with fusion experiments, so the same transfected CHO-K1 cells used for the fusion assays were used to analyze the cell surface expression of gB. For cELISAs associated with B cell fusion experiments, WT gB or gB CTD truncation mutants were coexpressed with the EBV glycoproteins gp42 and gH/gL. As described in the introduction, there was little WT gB detected at the cell surface. The shortest truncation mutants, gB757, gB767, gB772, gB776, and gB781, had very high cell surface expression compared to that of WT gB, in some cases nearly 10-fold higher cell surface expression than WT gB (Fig. 2A). In the central region of the CTD, the previously generated gB798 and gB801 mutants as well as the newly generated mutants from gB802 to gB839 all had intermediate levels of cell surface expression compared to the first group of short-length CTD mutants yet still significantly greater surface expression than WT gB (Fig. 2A). Mutants gB802 and gB803 had somewhat lower cell surface expression than other mutants within the central portion of the CTD. With the previously generated mutant gB841S, there was a shift in cell surface expression to levels much lower than those of any other mutants with truncations flanking this region, with a cell surface expression similar to that of WT gB (Fig. 2A). At the

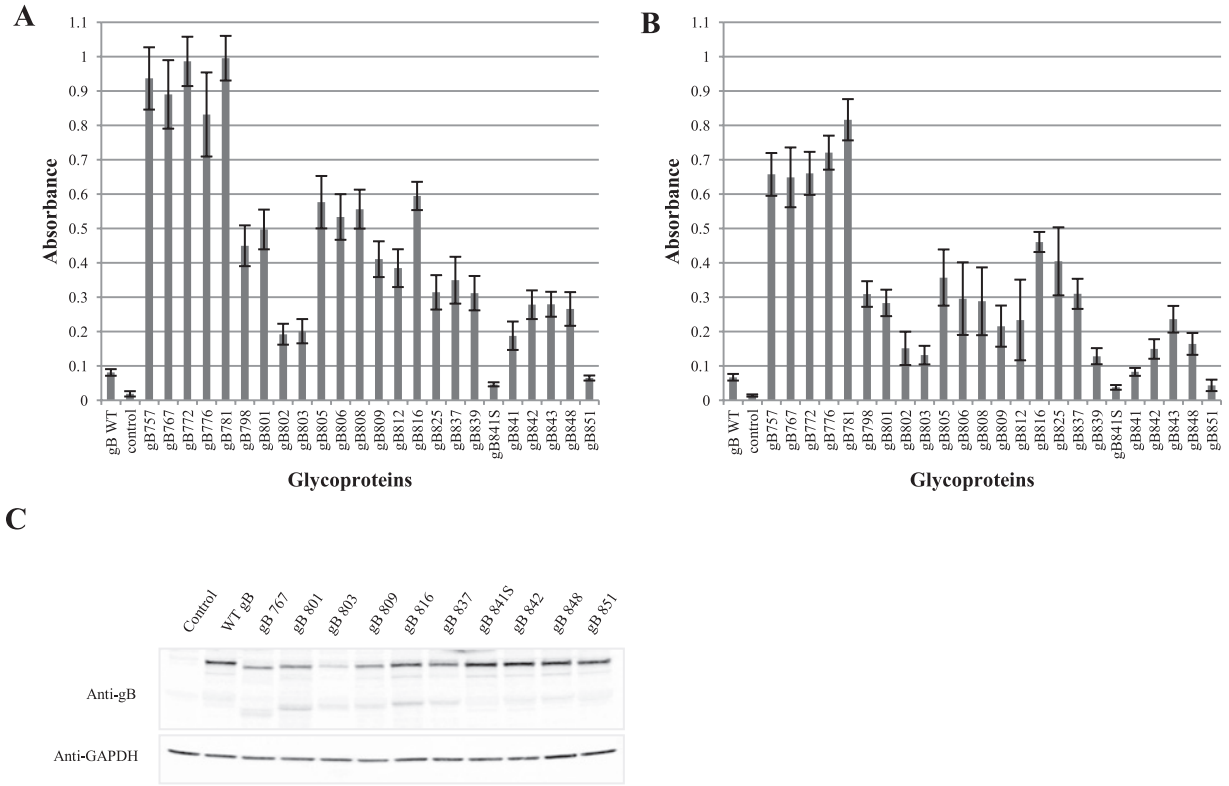

FIG 2 Expression of EBV gB CTD mutants via cell enzyme-linked immunosorbent assay (cELISA) and in whole-cell lysates. CHO-K1 cells were transfected and processed for cELISA in conjunction with cell-cell fusion experiments, as described in Materials and Methods. After transfection, cells were plated in 96-well plates in two sets of triplicates. Anti-EBV gB mouse monoclonal antibody CL55 was utilized to label gB cell surface expression. Data are representative of at least three independent experiments for each mutant. The control column is the vector control. Error bars indicate standard error calculations. (A) cELISA associated with B cell target fusion experiments (CHO-K1 cells also coexpress gH/gL and gp42). (B) cELISA associated with epithelial target fusion experiments (CHO-K1 cells also coexpress gH/gL). (C) CHO-K1 cells were transfected and processed for Western blot analysis under reducing conditions as described in Materials and Methods. The control lane is the vector control, and 110-kDa full-length wild-type EBV gB serves as a positive control. Mutants were selected on the basis of their inclusive phenotypic representation of proximal CTD length mutants. There is a slight shift in the molecular weights of mutants in line with the amount of amino acids truncated from the CTD. GAPDH served as a loading control.

end of the CTD, mutants gB841 through gB848 had intermediate cell surface expression compared to that of the short-length CTD mutants, such as gB767, but were still expressed at the cell surface to significantly greater levels than WT gB (Fig. 2A). Mutant gB851, with the longest CTD of the mutants studied (only 6 amino acids were deleted from the CTD), had cell surface expression similar to that of WT gB (Fig. 2A).

For cELISAs performed in conjunction with epithelial cell fusion experiments, WT gB or gB CTD mutants were coexpressed with gH/gL. In general, the cell surface expression trends associated with epithelial cell fusion experiments (Fig. 2B) reflect the same trends as described above for cell surface expression when gB is coexpressed with gp42 and gH/gL (Fig. 2A) and indicate that gp42 expression has little effect on the expression of gB.

A representative panel of mutants was chosen for Western blot analysis (Fig. 2C). Western blotting of whole-cell lysates revealed that all gB CTD mutants, with the exception of gB803, were expressed similarly to WT gB. The gB803 mutant, along with the gB802 mutant, was also expressed at lower levels in cELISAs (Fig. 2A and B), indicating that this is a general property of these two mutants.

Subcellular localization of EBV gB CTD mutants. In order to examine the subcellular localization of the gB CTD mutants, we performed confocal microscopy on an expanded panel of the mutants that we used for Western blot analysis (Fig. 3). WT gB had diffuse subcellular localization with pronounced perinuclear decoration. Mutants gB767, gB798, gB801, gB809, and gB816 did not have any pronounced perinuclear staining, unlike WT gB. Furthermore, these mutants did not appear to be as diffusely expressed subcellularly as WT gB; rather these gB CTD mutants were expressed in pronounced, punctate dots, which may represent clustered gB. Images of truncation mutant gB837 reveal a restoration of perinuclear decoration, although the perinuclear staining is not quite as robust as the perinuclear staining observed for WT gB. Also, the remaining subcellular gB of gB837 still manifested in somewhat punctate clusters. Truncation mutant gB839 continuing to mutant gB848 had considerable perinuclear staining, but it was still not as pronounced as observed with WT gB. However, the remaining subcellular expression of these mutants appeared to be diffuse, as for WT gB, not punctate. Truncation mutant gB851, the truncation mutant with the longest CTD, had considerable perinuclear decoration and diffuse expression throughout the rest of the cell. Overall, the observed results indicate that the gB CTD is important in regulating the cellular localization of gB.

Function of EBV gB CTD truncation mutants in fusion. Next, we examined the functional properties of the gB CTD mu-

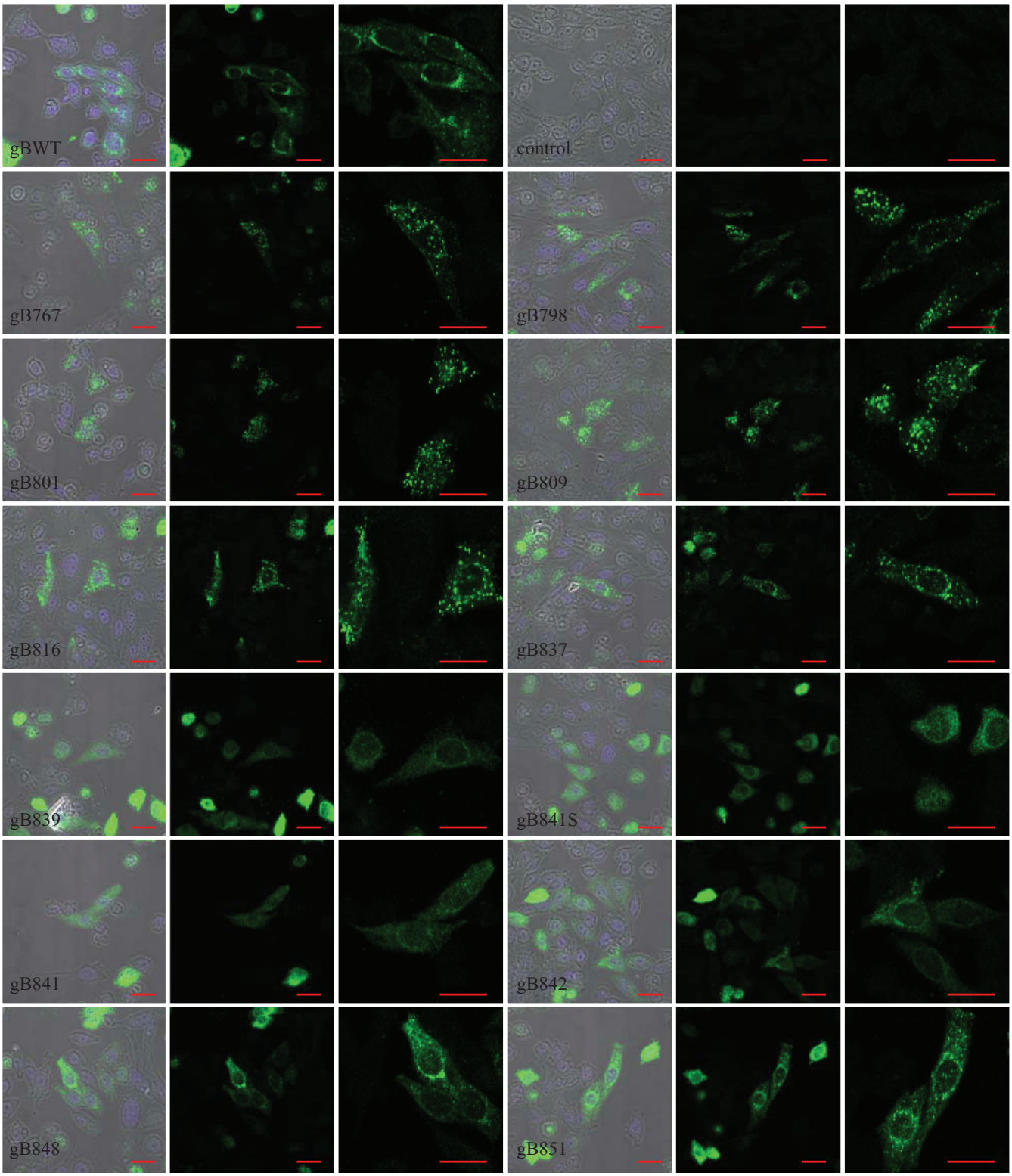

FIG 3 Altered localization of EBV gB CTD mutants analyzed via laser-scanning confocal microscopy. CHO-K1 cells were transfected with a representative panel of gB CTD mutants and plated on coverslips as outlined in Materials and Methods. Cells were fixed in methanol and incubated with anti-EBV gB mouse monoclonal antibody CL55 and then with goat anti-mouse IgG AlexaFluor488-conjugated secondary antibody. Coverslips were mounted on slides using ProLong Gold antifade mounting medium with DAPI. Images were captured with a ×63 magnification oil immersion objective on a Zeiss UV-LSM510 confocal microscope. For each representative mutant, the leftmost panel depicts a phase-contrast image overlaid with DAPI labeling and AlexaFluor488 labeling of gB expression. The middle panels depict only gB expression, and the rightmost panels are zoomed-in sections of each middle panel. Red scale bars represent 20 μm in each respective image panel.

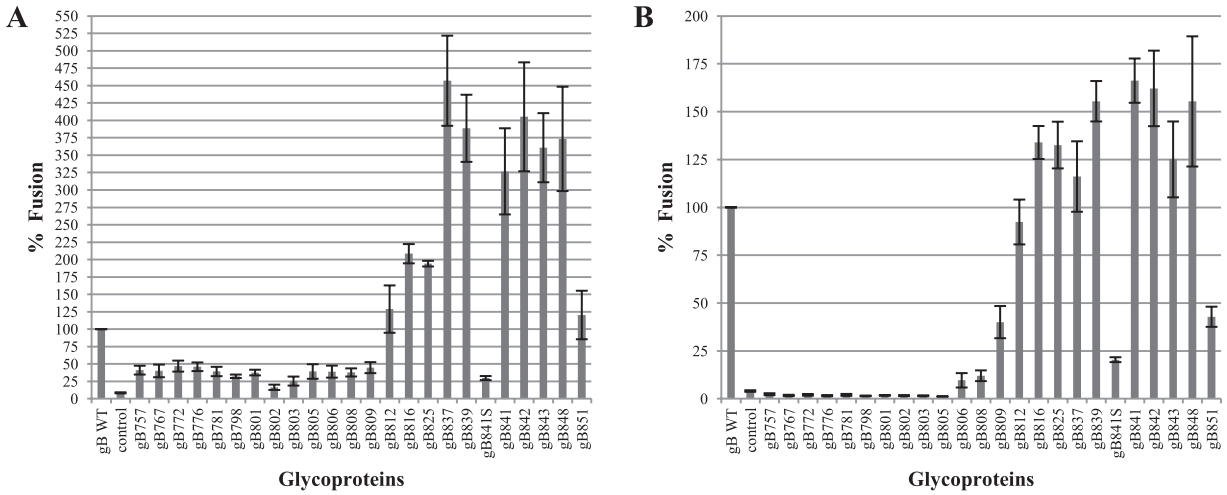

FIG 4 EBV gB CTD mutants exhibit similar patterns of fusion activity in both B cell and epithelial cell targets. CHO-K1 cells were transfected as described in Materials and Methods. Briefly, CHO-K1 effector cells were transfected with plasmids encoding T7 luciferase under the control of the T7 promoter, EBV gH/gL, and WT gB or mutant gB CTD constructs. EBV gp42 is also cotransfected in effector cells used for B cell target fusion experiments but not for effector cells used in epithelial cell target fusion experiments. Cells were overlaid with 293T14 epithelial cell target cells (A) or Daudi-29 B cell target cells (B), both of which stably express T7 RNA polymerase. After coincubation of effector and target cells, luciferase activity was measured and is indicative of relative cell-cell fusion. Fusion mediated by WT gB coexpressed with other necessary EBV glycoproteins (gH/gL for epithelial cell target fusion experiments; gp42 and gH/gL for B cell target fusion experiments) is set to 100%, and all other fusion readouts are compared to this reading. Data are averages of results from at least three experiments per construct. Control columns are those with the vector control. Error bars represent standard errors.

tants using a cell-based fusion assay. This assay allows quantitative examination of fusion function without having to use virus, thereby creating a simplified background for analysis. Mutants with the largest CTD truncations, such as gB757, gB772, and mutants up to gB809, were hypofusogenic (in this study, "hypofusogenic" refers to mutants with fusion phenotypes above background levels up to 90% of the fusion levels observed with WT gB) in epithelial cell fusion compared to WT gB (Fig. 4A). The truncation mutant gB812 was hyperfusogenic (in this study, "hyperfusogenic" refers to mutants with fusion phenotypes above 110% of the fusion levels observed for WT gB) and this hyperfusogenic phenotype was maintained for mutants through gB839. Mutant gB812 separates the bulk of hypofusogenic CTD truncation mutants from hyperfusogenic CTD truncation mutants. With mutant gB841S, there was a shift from a hyperfusogenic phenotype to that of a hypofusogenic phenotype compared to WT gB. Interestingly, mutant gB841, without the two additional nonendogenous amino acids found in gB841S through gB848 had a restoration of a hyperfusogenic phenotype. Mutant gB851, the mutant with the longest CTD, had a slight hyperfusogenic phenotype.

The phenotypic trends of fusion with B cell targets (Fig. 4B) paralleled the trends described above for fusion with epithelial cell targets (Fig. 4A). The shortest mutants, such as gB757, gB767, and mutants through gB805, were essentially fusion null (in this study, "fusion null" refers to mutants with fusion phenotypes at or below background levels), mediating little-to-no fusion with B cell targets (Fig. 4B). The behavior for these mutants is slightly different than what was observed in epithelial cell fusion experiments, where the mutants were able to mediate fusion levels above background but were still hypofusogenic compared to WT gB. Mutants gB806 through gB809 exhibited fusion levels above background but were still hypofusogenic. Mutant gB812 was WT-like (in this study, "WT-like" refers to mutants with fusion phenotypes that were 90% to 110% of fusion levels observed with WT gB) in fusion with B cell targets, rather than mildly hyperfusogenic, as in epithelial cell fusion. However, truncation mutant gB812 separated the majority of fusion-null and hypofusogenic CTD truncation mutants from the hyperfusogenic CTD truncation mutants, similar to observations of fusion with epithelial cell targets. Mutants gB816 through gB839 were hyperfusogenic, and as with the findings for epithelial cell fusion, there was a sharp reduction in fusion to levels below levels observed with WT gB for gB841S. Fusion was restored to a hyperfusogenic state with mutants gB841 through gB848, with reduction to below WT gB levels of fusion for mutant gB851. Mutant gB851 in this case was clearly hypofusogenic, not slightly hyperfusogenic compared to WT gB, as seen in epithelial fusion experiments.

DISCUSSION

Past studies examining gB homologues across the herpesvirus α, β, and γ subfamilies have shown that the gB CTD plays a role in the regulation of fusion and gB subcellular localization. Led by early studies showing that mutating the HSV (herpes simplex virus) gB CTD caused syncytium formation in virus-infected cells (26), researchers later demonstrated that mutating the CTD of HSV gB can both positively and negatively regulate fusion (27–41). The gB of another alphaherpesvirus, pseudorabies virus (PrV), also has an altered fusion phenotype when its CTD is mutated (42). In the β subfamily, deletion mutations introduced in the CTD and transmembrane domain of human cytomegalovirus (HCMV) gB led to either impaired or little-to-no syncytium formation, which is typically observed with cells expressing WT gB, suggesting that a role of the HCMV gB CTD is fusion regulation (43, 44). Additionally, a virus of the γ subfamily, human herpesvirus 8 (HHV-8), also expresses a gB homologue, and when the HHV-8 gB CTD is mutated, its fusion phenotype is altered (45).

As previous studies with EBV gB have demonstrated, the EBV gB CTD appears to play an important role in regulating fusion

with lymphocytes and epithelial cells. However, the regions of the CTD which are responsible for fusion regulation and the manner in which the properties of the CTD allow for regulation are not well understood. Through the creation of a library of CTD truncation constructs, we were able to further determine specific regions of the tail that are important for fusion regulation as well as for the expression and localization pattern of EBV gB. There are, however, multiple explanations for the phenotypes observed in our studies. Both the previously generated gB CTD mutant constructs (gB798, gB801, gB816, and gB841S) and the more comprehensive constructs generated for this study can be generally divided into three classes based on their phenotypes in cell-cell fusion and cell surface expression. With regard to fusion, mutants are fusion null (at or below background levels of fusion), hypofusogenic (above background levels to 90% of the fusion levels observed with WT gB), WT-like (90 to 110% of the fusion levels observed with WT gB), or hyperfusogenic (above 110% of the fusion levels observed with WT gB). In terms of expression, mutants can be characterized as being expressed at a low level at the cell surface, like WT gB (or below WT levels of expression), intermediately expressed at the cell surface (moderately above WT levels of surface expression), or highly expressed at the cell surface.

Class I EBV gB CTD constructs. Class I mutants are categorized based on high cell surface expression and low levels of fusion observed with B cell and epithelial target cell types. Constructs gB757, gB767, gB772, gB776, and gB781 are expressed more highly at the cell surface than any other characterized mutants, with levels approaching 10-fold more than WT levels for some constructs. However, these mutants are null in mediating fusion with B cell targets and hypofusogenic with epithelial cell targets.

Class II EBV gB CTD constructs. Class II mutants are categorized based on intermediate cell surface expression (greater than that of WT gB, which is expressed at a low level on the cell surface) with either null, hypofusogenic, WT-like, or hyperfusogenic levels of fusion with B cell or epithelial target cell types. Constructs gB798, gB801, gB802, gB803, and gB805 are null in B cell fusion, with closely related gB806, gB808, and gB809 mediating slight levels of fusion as the CTD length increases. All of these mutants are hypofusogenic in mediating fusion with epithelial targets. It is interesting that the majority of the observed fusion-null and hypofusogenic phenotypes result from truncating the CTD past gB812 but that the majority of constructs longer in CTD length than gB812 are hyperfusogenic. Thus, in general, gB812 can be thought of as separating the truncation mutants with hyperfusion phenotypes from those with fusion-null or hypofusogenic phenotypes. Constructs gB816, gB825, gB837, gB839, gB841, gB842, gB843, and gB848 are hyperfusogenic for both target cell types.

Class III EBV gB CTD constructs. Class III mutants are characterized by a low cell surface expression (similar to that of WT gB or below WT-gB levels of cell surface expression) and hypofusogenic or slightly hyperfusogenic in terms of their ability to mediate fusion with both target cell types. Construct gB841S mediates very low levels of fusion and is poorly expressed on the cell surface. It is possible that the inability of this mutant to mediate moderate levels of fusion is due to a trafficking defect. Construct gB851, which also has a WT-like level of cell surface expression, is hypofusogenic with B cell targets and yet slightly hyperfusogenic with epithelial cell targets.

Subtle differences in fusion levels observed between B cell targets and epithelial cell targets may be reflective of the sensitivity of the cell fusion assay and related to target B cells growing in suspension, unlike target epithelial cells, which are adherent, like adherent CHO-K1 EBV glycoprotein-expressing effector cells (as observed in reference 22).

Many possible explanations exist with regard to the fusion phenotypes observed with the EBV gB CTD truncation constructs, including altering the presence of putative endocytosis motifs located in the CTD, altering a potential trimerization domain in the CTD, and influencing the secondary structure of the CTD and its potential association with membranes. Also, altering the structure/conformation of the gB ectodomain, which is thought to be physically responsible for fusing virus and cell membrane, may also account for differences in fusion function.

gB CTD putative endocytosis motifs and gB fusion function. Of the variety of characterized endocytosis motifs, most pertinent to the current study are tyrosine-based motifs (YXXΦ) (X represents any amino acid, although Y + 2 is commonly an arginine, and Φ represents a large hydrophobic amino acid) and dileucine-based (LL) motifs (46). These motifs appear in the gB CTDs of PrV (47), HHV-8 (45), and HSV-1 and -2 (39–41), as well as among other viral proteins and cellular proteins. When the HHV-8 gB CTD is truncated by 58 residues, which removes a YXXΦ and an LL motif, there is a shift in expression of gB from predominantly perinuclear expression to expression on the cell surface, also resulting in increased cell fusion (45). Similarly, the cellular localization of HSV-2 gB was influenced by the presence of potential endocytosis motifs in the CTD; however, the degree of cell surface expression of these mutants did not necessarily correlate with the levels of fusion associated with these mutants (39).

There are three putative endocytosis motifs in the EBV CTD: YPGI (residues 768 to 771), YHDP (residues 840 to 843), and LL (residues 849 to 850) (Fig. 1C, indicated in bold in the primary amino acid sequence); however, whether or not these motifs function as endocytosis motifs for EBV gB is not well understood. If these residues in fact function as endocytosis motifs for EBV gB, mutating the residues may increase the level of gB at the cell surface, which would in turn increase the potential for fusion to occur. However, truncating the most TM-proximal putative endocytosis motif, YPGI (as with mutant gB767), as well as considering the class I mutants (gB757 to gB781), which bound this motif, resulted in high cell surface expression of gB yet fusion-null or hypofusogenic fusion phenotypes. This finding, as well as others from our current study, is supportive of the notion that cell surface expression is not alone a determinant for fusion (21, 22, 29, 39, 40, 48).

The next motif, YHDP, may not necessarily constitute an endocytosis motif (on the basis of the hydrophobicity of proline); however, noncanonical motifs have also been shown to also mediate endocytosis, like their canonical counterparts (49, 50). This putative noncanonical motif flanks the arginine repeat domain of the CTD. As our previous studies have suggested that local configuration and structural features around this motif may influence gB localization (20), we generated a number of constructs with truncations in this area which are members of class II and class III mutant designations. The previously generated mutant gB841S, a class III mutant, introduced two additional amino acids (arginine and leucine) onto the truncated endogenous sequence as a result of cloning manipulations. These additional amino acids added to the end of amino acid 841 (histidine) of the CTD created a nonendogenous YHRL motif (Fig. 1C), and perhaps the low expres-

sion of this mutant may be a result of the addition of this motif, which may explain the low levels of fusion observed. However, it is also possible that this protein is misfolded and poorly translocated to the cell surface. The other mutants flanking the putative noncanonical endogenous YHDP motif belong to class II. Constructs with truncations before and after YHDP, such as constructs between those of gB837 and gB848, show little difference in their intermediate levels of surface expression and hyperfusogenicity, suggesting that the YHDP sequence likely does not serve as an endocytosis motif that could hypothetically play a role in the cell surface expression of gB and in turn in the potential fusion function of gB.

The putative LL motif located between residues 849 and 850 may account for the differences between the strongly hyperfusogenic class II mutant gB848 and the hypofusogenic (in B cells) and slightly hyperfusogenic (in epithelial cells) class III mutant gB851. The LL motif is present in gB851, which has WT-like levels of surface expression. However, gB848, which truncates the LL motif, has a slight increase in cell surface expression as well as a considerable increase in fusion function. Nevertheless, taking into account our hypothesis that cell surface expression does not directly correlate with levels of fusion regulated by the gB CTD and the fact that we are unsure of the functional nature of these motifs in the EBV gB CTD, more work must be done to understand their importance.

gB CTD trimerization motifs and gB fusion function. Recently, the ectodomains of HSV-1 and EBV gB were crystallized and determined to form trimers (11, 12). Interestingly, oligomerization of EBV gB appears to be important for the ability of EBV gB to mediate fusion with B cell and epithelial cells targets, as linker insertion mutations disrupting oligomerization of gB fail to permit fusion (23).

Size exclusion chromatography elution profiles suggest that the EBV gB CTD elutes as a trimer in buffer, which presents the possibility of a trimerization domain located in the CTD (51). Parallel size exclusion chromatography studies with the HSV-1 gB CTD reveal that both the full-length CTD and truncated CTD constructs exist as trimers in solution, suggesting that there is a trimerization domain located between gB residues 801 and 851 (52). It would be interesting to test our panel of truncation mutants using similar techniques, not only to better understand the sequence-based context of the potential trimerization domain but also to clarify how the potential trimerization domain located in the CTD may impact fusion.

gB CTD membrane interaction and gB fusion function. Several recent studies have focused on the interaction of the gB CTD with membranes. The EBV gB CTD complexes with membrane mimics upon being mixed. This interaction corresponds to a structural change resulting in an increase in α-helical content (51), compatible with the predicted secondary structure of the CTD, in which α-helical regions are predicted (24, 25, 51) (Fig. 1B). Similarly, recent studies with the full-length WT HSV-1 gB CTD have shown that there is an increase in helicity of the CTD in a membrane-mimetic environment compared to that in an aqueous buffer environment, indicating that disordered regions of the gB CTD fold into helical regions as a result of their interaction with membrane mimics (52). Interestingly, compared to purified WT CTD, purified truncated CTD constructs corresponding to previously characterized full-length HSV-1 gB constructs with CTD truncations known to alter the fusion phenotype (27, 28, 32, 52) had a decrease in helical transition in membrane mimics and a decrease in binding to membrane mimics, suggesting that stable membrane interaction of the gB CTD may regulate fusion and implying that α-helical regions of the CTD may be necessary for this membrane interaction (52).

Interestingly, there was no reduction in binding to membrane mimics of purified point mutant CTD constructs corresponding to previously characterized full-length HSV-1 gB proteins with syncytial point mutations (28, 35, 36) compared to that of the WT gB CTD (48). Intriguingly, some bound better than the WT CTD (48) when mixed with membrane mimics, and had increases in α-helical content similar to that of the WT CTD, indicating that there is not a direct relationship between membrane binding and the degree of helical transition of the CTD in a membrane environment (48).

When mixed with membrane mimics, the WT HSV-1 CTD had a dramatic reduction in protease sensitivity compared to that in buffer solution, indicating that a large portion of the CTD formed a proteolytically shielded core in a membrane environment. This was similarly observed for the point mutant syncytial CTD constructs, yet with some slight differences (48). Taking into account these differences and similar stabilities of the WT CTD and syncytial point mutant CTDs in denaturing urea, this suggested that these mutations in the CTD result in local rather than global conformational changes in the membrane-bound CTD (48). It was postulated that these local conformational changes may disturb intramolecular CTD interactions that would otherwise be present in the WT CTD, resulting in a shift from WT CTD membrane-bound conformation and thereby causing fusion deregulation (48).

As a result of the complexity of the fusion phenotypes that we observed when mutating the EBV CTD and the lack of a crystal structure of the CTD, it is difficult to imply particular helical regions of the CTD in regulating fusion. However, based on secondary-structure prediction and noting that the bulk of our fusion-null and hypofusogenic phenotypes were observed for mutants with truncations in the CTD past gB812 (the bulk of our hyperfusogenic phenotypes were observed for mutants with CTDs longer than in gB812), it is possible that the two most-C-terminal helical regions in the predicted structure may be important in negatively regulating fusion. However, whether or not this regulation is through an association with membrane or due to gB812-gB857 being a domain of the CTD with important fusion-antagonizing intramolecular interactions will require future studies.

gB CTD alteration of ectodomain conformation and gB fusion function. Previous studies with paramyxovirus simian virus 5 (SV5) F protein have shown that the length of the CTD can have dramatic effects on fusion function. Some SV5 F proteins from different viral isolates also differ in CTD length, with the F proteins with shorter CTDs mediating high levels of fusion and F proteins with longer CTDs causing little-to-no detectable syncytia (53, 54). Truncating the CTDs of longer CTD F proteins to the same length as the CTDs of shorter F protein isolates results in fusion levels similar to those observed with shorter CTD F proteins (53, 54). SV5 F protein isolates can have different reactivities to conformationally specific antibodies depending on CTD length or the presence of mutations (55, 56), indicating that the SV5 CTD can regulate the conformation of the F protein ectodomain (57). Additional studies extending the CTD of a short SV5 F protein

isolate or adding tags that allow the formation of a 3-helix bundle to the CTD suggested that these additions increase intramolecular interactions that stabilize the F protein in a prefusion form (57). As the SV5 F protein TMs must rotate in the plane of the membrane during the conformational transition from prefusion to postfusion form, the effects of stabilizing the CTD of the F protein may restrict the ability of TMs to rotate, thereby affecting the ability of the ectodomains to interact, fold, and otherwise alter their conformations (57).

Interestingly, no significant conformational differences were observed between syncytial HSV-1 gB CTD mutants and WT gB using a panel of conformational antibodies specific to ectodomain epitopes (48). However, it is not possible to rule out the possibility that there may be small conformational changes in the ectodomain which could not be detected with the antibodies utilized in this study or that the appropriate conformation-specific antibodies have not been identified.

In the case of the EBV gB CTD, it is possible that the CTD truncations in our study potentially cause a conformational change that travels through gB, ultimately affecting the conformation of the ectodomains, rendering them either more or less fusogenic, and altering the energy threshold for the conversion of gB from a pre- to a postfusion form. As noted earlier, the bulk of observed fusion-null and hypofusogenic EBV gB CTD truncation constructs are clustered before gB812, whereas the bulk of our hyperfusogenic constructs have CTDs longer than that of gB812. In-line with the reasoning of the SV5 F protein study described above (57), this suggests that truncating the EBV CTD up to position 812 removes conformational restrictions that would otherwise increase the energy threshold for fusion, allowing conformational changes to be transmitted through the protein and rendering the ectodomain more fusogenic. However, without a panel of conformational antibodies specific to EBV gB ectodomains, it is difficult for us to assess whether or not mutations in this region or other regions of the EBV gB CTD alter the conformation of the gB ectodomains and, as a result, possibly alter the fusogenic potential of the ectodomains. Further studies directed at understanding the function of EBV gB in fusion are clearly warranted, with the mutants described in this study providing a basis for future research.

MATERIALS AND METHODS

Cells and antibodies. Cells were cultured in media supplemented with 10% serum (fetal bovine serum [Atlanta Biologicals] or FetalPlex [Gemini Bioproducts]) and 1% streptomycin-penicillin (100 U penicillin/ml, 100 μg streptomycin/ml) (Sigma).

CHO-K1 cells were cultured in Ham's F-12 medium (Mediatech-Cellgro/ThermoFisher-HyClone). Daudi-29 cells (stably expressing T7 RNA polymerase) (as described in reference 58) were cultured in RPMI medium (Mediatech-Cellgro) containing 900 μg/μl Geneticin/G418 sulfate (Gibco-Invitrogen). 293T14 cells (stably expressing T7 RNA polymerase) (as described in reference 59) were cultured in Dulbecco's modified Eagle's medium (DMEM) (Mediatech-Cellgro) containing 100 μg/ml zeocin (Invitrogen).

The mouse monoclonal EBV gB antibody CL55 was kindly provided by Lindsay Hutt-Fletcher (60) (Louisiana State Health Sciences Center, Shreveport, LA). Rabbit polyclonal EBV gB antibody was produced by immunizing rabbits with EBV gB expression vectors (Aldevron). Mouse monoclonal GAPDH (glyceraldehyde-3-phosphate dehydrogenase) antibody was purchased from Abcam. Biotinylated goat anti-mouse IgG conjugate was purchased from Sigma. Streptavidin-horseradish peroxidase conjugate was purchased from GE Healthcare.

EBV gB CTD truncation mutant generation. The EBV gB CTD truncation mutants were created using the QuikChange site-directed mutagenesis kit (Stratagene). Primers were designed based on the sequence of WT EBV gB in the pSG5 vector (Stratagene) as a template. As we desired to create a comprehensive library of mutant constructs, forward and reverse primers were designed to incorporate stop codons in the gB CTD to generate truncations ranging from the TM-proximal region of the CTD to near the C terminus of the CTD. Sequencing analysis was performed to confirm the appropriate truncation mutations in the CTD (Northwestern Genomics Core Facility).

Transfection. CHO-K1 cells were plated in 6-well tissue culture plates (BD-Falcon) 1 day prior to transfection, such that the cells were subconfluent at the time of transfection. CHO-K1 cells were transfected using Lipofectamine 2000 (Invitrogen). At the time of transfection, CHO-K1 cells seeded in 6-well plates were washed once with phosphate-buffered saline (PBS) and then placed in Opti-MEM reduced-serum medium (Gibco). For epithelial-fusion-related experiments, 0.8 μg of EBV gH, 0.8 μg of EBV gL, 0.8 μg of the T7 promoter-driven luciferase reporter expression vector, and 0.8 μg of either WT EBV gB or EBV gB CTD truncation mutant DNA were combined with Lipofectamine 2000 and incubated for 30 min in a total volume of 500 μl of Opti-MEM prior to being added to cells. For B cell fusion experiments, 2.0 μg of EBV gp42, 0.8 μg of EBV gH, 0.8 μg of EBV gL, 0.8 μg of the T7 promoter-driven luciferase reporter expression vector, and 0.8 μg of either WT EBV gB or EBV gB CTD truncation mutant DNA were combined with Lipofectamine 2000 and incubated for 30 min in a total volume of 500 μl of Opti-MEM prior to being added to cells. Cells were incubated overnight with the transfection mixture, and in the morning, the transfection mixture was removed and replaced with Ham's F-12 medium supplemented with 10% fetal bovine serum (FBS) and 1% streptomycin-penicillin (100 U penicillin/ml, 100 μg streptomycin/ml) prior to use in experiments.

Fusion assay. The virus-free, cell-based fusion assay was carried out as previously described (21, 22). Effector CHO-K1 cells for epithelial fusion experiments were transiently transfected with EBV gH/gL, the T7 promoter-driven luciferase reporter expression vector, and either WT EBV gB or EBV gB CTD mutants as outlined above. Effector CHO-K1 cells for B cell fusion experiments were transiently transfected with EBV gp42, EBV gH/gL, the T7 promoter-driven luciferase reporter expression vector, and either WT EBV gB or EBV gB CTD mutants as outlined above. For epithelial and B cell fusion experiments, target cells were 293T14 and Daudi-29 cells, respectively. After an overnight transfection, cells were detached from plates using 1 mM EDTA diluted in PBS and counted with a Beckman-Coulter Z1 particle counter. CHO-K1 effector transfectants (2.5×10^5) were added to an equal amount of 293T14 or Daudi-29 cells in a total volume of 1 ml of Ham's F-12 medium in a 24-well plate (BD Falcon). Approximately 22 to 24 h later, cells were washed once with PBS and lysed with 100 μl of passive lysis buffer (Promega) diluted in PBS. To quantify fusion, luciferase activity was measured in duplicate by adding 20 μl of lysed cells to a treated 96-well tissue culture IsoPlate (PerkinElmer) and by adding 100 μl of luciferase assay reagent (Promega); luminescence was then read on a Wallac Victor^2 multilabel plate reader (PerkinElmer).

cELISA. The same experimental populations of CHO-K1 cells expressing EBV glycoproteins which were utilized for fusion assays were analyzed for cell surface expression of EBV gB via a cell ELISA (cELISA). At the time that the transfected CHO-K1 effector cells were overlaid with target cells, a portion of the CHO-K1 cells were plated 4×10^4 cells per well in two sets of triplicates (one set of triplicates for experimental readout and the other set of triplicates for background calculations) in a 96-well plate. After approximately 22 to 24 h, cells were washed once with PBS and incubated for 30 min with CL55 mouse monoclonal antibody directed against EBV gB diluted 1:200 in 3% bovine serum albumin (BSA) (Sigma) in PBS supplemented with $MgCl_2$ and $CaCl_2$ (PBS-ABC) (experimental triplicate set) or incubated in only 3% BSA in PBS-ABC (control

triplicate set). Cells were then washed five times with PBS-ABC and then fixed for 10 min in a solution of 2% formaldehyde (Fisher) and 0.2% glutaraldehyde (Sigma) in PBS-ABC. Following fixation, cells were washed three times in 3% BSA in PBS-ABC. Next, cells were incubated for 30 min with biotinylated goat anti-mouse IgG conjugate (Sigma) diluted 1:500 in 3% BSA–PBS-ABC and then washed five times before a 30-min incubation with streptavidin-horseradish peroxidase conjugate (GE Healthcare) diluted 1:20,000 in 3% BSA in PBS-ABC. Following five washes in 0.1% Tween 20 (Fisher) diluted in PBS-ABC, TMB One Component horseradish peroxidase microwell substrate (BioFX Laboratories) was added to each well and allowed to incubate for 15 to 20 min. The resulting color change reaction was read with a PerkinElmer Wallac Victor^2 multilabel plate reader.

Western blotting. A representative subset of the EBV gB CTD mutants was selected for Western blot analysis. In a 6-well tissue culture plate (BD-Falcon), CHO-K1 cells were plated at a density of 2.5×10^5 cells per well and transfected with 2.0 μg of WT EBV gB or gB CTD mutant DNA overnight. In the morning, cells were washed twice with ice-cold PBS and lysed in 250 μl of 1× Laemmli sample buffer (Bio-Rad). Lysates in Laemmli sample buffer were collected in microcentrifuge tubes, sonicated, and then boiled at 95°C for 5 min. Samples were then loaded and run on Any kD Mini-Protean TGX gels (Bio-Rad). After electrophoresis, samples were transferred to nitrocellulose membranes (Whatman). After transference, membranes were blocked in 5% nonfat dry milk in TBS buffer (20 mM Tris-HCl [pH 7.6], 137 mM NaCl) for 1 h at room temperature. After three washes in TBS, blots were incubated overnight at 4°C with EBV gB rabbit polyclonal antibody diluted 1:1,000 in 5% BSA in TBS and anti-GAPDH mouse monoclonal antibody diluted 1:1,000. Next, blots were washed three times in TBS and then incubated for 1 h with anti-rabbit secondary antibody conjugated to IRDye 800 (LI-COR) diluted 1:10,000 in 5% BSA in TBS or anti-mouse secondary antibody conjugated to IRDye 680 (LI-COR) diluted 1:10,000. Following secondary antibody incubation, the blots were washed three times in TBS and the infrared emission of bands corresponding to lanes of loaded lysates was read on the LI-COR Odyssey Fc machine.

Confocal microscopy. CHO-K1 cells were seeded in 6-well tissue culture plates (BD-Falcon) at a density of 3.0×10^5 cells per well 1 day prior to transfection. Lipofectamine 2000 transfection reagent was mixed with 0.8 μg of WT EBV gB or gB CTD mutant DNA, 0.8 μg of EBV gH DNA, and 0.8 μg of EBV gL DNA in Opti-MEM medium. Cells were incubated overnight in the transfection mixture. In the morning, cells were washed once with PBS and detached using 1 mM EDTA diluted in PBS and then counted using a Beckman Coulter Z1 particle counter. Prior to being seeded, the glass coverslips were treated with poly-L-lysine (Sigma) and washed twice with PBS and once with Ham's F-12 medium. Cells from each well were seeded on glass coverslips in a treated 12-well tissue culture plate (BD-Falcon) and allowed to spread for 24 h. Then, cells were washed once with PBS and fixed in ice-cold methanol for 10 min. Following fixation, cells were placed in a blocking solution consisting of 5% goat serum (Sigma) diluted in PBS. Next, cells were washed three times with PBS and incubated for 1 h at room temperature in CL55 anti-EBV gB mouse monoclonal antibody diluted 1:250 in 3% BSA in PBS. After being washed three times in PBS, cells were incubated for 1 h at room temperature in goat anti-mouse IgG AlexaFluor488-conjugated secondary antibody (Invitrogen) diluted 1:1,000 in 3% BSA in PBS. After being washed three times in PBS, the coverslips were mounted on slides using ProLong Gold antifade mounting medium with DAPI (4',6-diamidino-2-phenylindole) (Molecular Probes/Invitrogen). Images were captured with a ×63 magnification oil immersion objective on a Zeiss UV-LSM510 confocal microscope.

ACKNOWLEDGMENTS

This research was supported by grants AI076183 (R.L.) and AI067048 (R.L. and N.J.G.) from the National Institute of Allergy and Infectious Diseases, CA117794 (R.L.) from the National Cancer Institute, and 12POST9380013 from the American Heart Association (J.C.).

We appreciate the help and advice from other members of the Longnecker laboratory for the completion of these studies. We thank Lindsey Hutt-Fletcher for kindly providing monoclonal antibodies used in these studies. Imaging work was performed at the Northwestern University Cell Imaging Facility, generously supported by NCI CCSG grant P30 CA060553 awarded to the Robert H. Lurie Comprehensive Cancer Center. EBV gB CTD construct sequencing was performed by the Northwestern Genomics Core Facility.

REFERENCES

1. **Rickinson AB, Kieff E.** 2007. Epstein-Barr virus, p 2657–2701. *In* Knipe DM, Howley PM, Griffin DE, Lamb RA, Martin MA, Roizman B, Straus SE (ed), Fields virology, 5th ed. Lippincott Williams & Wilkins, Philadelphia, PA.
2. **Babcock GJ, Decker LL, Volk M, Thorley-Lawson DA.** 1998. EBV persistence in memory B cells *in vivo*. Immunity **9**:395–404.
3. **Thorley-Lawson DA, Babcock GJ.** 1999. A model for persistent infection with Epstein-Barr virus: the stealth virus of human B cells. Life Sci. **65**: 1433–1453.
4. **Spear PG, Longnecker R.** 2003. Herpesvirus entry: an update. J. Virol. **77**:10179–10185.
5. **Connolly SA, Jackson JO, Jardetzky TS, Longnecker R.** 2011. Fusing structure and function: a structural view of the herpesvirus entry machinery. Nat. Rev. Microbiol. **9**:369–381.
6. **Pellett PE, Biggin MD, Barrell B, Roizman B.** 1985. Epstein-Barr virus genome may encode a protein showing significant amino acid and predicted secondary structure homology with glycoprotein B of herpes simplex virus 1. J. Virol. **56**:807–813.
7. **Backovic M, Leser GP, Lamb RA, Longnecker R, Jardetzky TS.** 2007. Characterization of EBV gB indicates properties of both class I and class II viral fusion proteins. Virology **368**:102–113.
8. **Rasile L, Ghosh K, Raviprakash K, Ghosh HP.** 1993. Effects of deletions in the carboxy-terminal hydrophobic region of herpes simplex virus glycoprotein gB on intracellular transport and membrane anchoring. J. Virol. **67**:4856–4866.
9. **Gong M, Ooka T, Matsuo T, Kieff E.** 1987. Epstein-Barr virus glycoprotein homologous to herpes simplex virus gB. J. Virol. **61**:499–508.
10. **Pereira L.** 1994. Function of glycoprotein B homologues of the family Herpesviridae. Infect. Agents Dis. **3**:9–28.
11. **Backovic M, Longnecker R, Jardetzky TS.** 2009. Structure of a trimeric variant of the Epstein-Barr virus glycoprotein B. Proc. Natl. Acad. Sci. U. S. A. **106**:2880–2885.
12. **Heldwein EE, Lou H, Bender FC, Cohen GH, Eisenberg RJ, Harrison SC.** 2006. Crystal structure of glycoprotein B from herpes simplex virus 1. Science **313**:217–220.
13. **Roche S, Bressanelli S, Rey FA, Gaudin Y.** 2006. Crystal structure of the low-pH form of the vesicular stomatitis virus glycoprotein G. Science **313**:187–191.
14. **Roche S, Rey FA, Gaudin Y, Bressanelli S.** 2007. Structure of the prefusion form of the vesicular stomatitis virus glycoprotein G. Science **315**: 843–848.
15. **Hannah BP, Cairns TM, Bender FC, Whitbeck JC, Lou H, Eisenberg RJ, Cohen GH.** 2009. Herpes simplex virus glycoprotein B associates with target membranes via its fusion loops. J. Virol. **83**:6825–6836.
16. **Hannah BP, Heldwein EE, Bender FC, Cohen GH, Eisenberg RJ.** 2007. Mutational evidence of internal fusion loops in herpes simplex virus glycoprotein B. J. Virol. **81**:4858–4865.
17. **Backovic M, Jardetzky TS, Longnecker R.** 2007. Hydrophobic residues that form putative fusion loops of Epstein-Barr virus glycoprotein B are critical for fusion activity. J. Virol. **81**:9596–9600.
18. **Gong M, Kieff E.** 1990. Intracellular trafficking of two major Epstein-Barr virus glycoproteins, gp350/220 and gp110. J. Virol. **64**:1507–1516.
19. **Lee SK, Longnecker R.** 1997. The Epstein-Barr virus glycoprotein 110 carboxy-terminal tail domain is essential for lytic virus replication. J. Virol. **71**:4092–4097.
20. **Lee SK.** 1999. Four consecutive arginine residues at positions 836–839 of EBV gp110 determine intracellular localization of gp110. Virology **264**: 350–358.
21. **Haan KM, Lee SK, Longnecker R.** 2001. Different functional domains in the cytoplasmic tail of glycoprotein B are involved in Epstein-Barr virus-induced membrane fusion. Virology **290**:106–114.
22. **McShane MP, Longnecker R.** 2004. Cell-surface expression of a mutated

Epstein-Barr virus glycoprotein B allows fusion independent of other viral proteins. Proc. Natl. Acad. Sci. U. S. A. **101**:17474–17479.
23. **Reimer JJ, Backovic M, Deshpande CG, Jardetzky T, Longnecker R.** 2009. Analysis of Epstein-Barr virus glycoprotein B functional domains via linker insertion mutagenesis. J. Virol. **83**:734–747.
24. **Buchan DW, Ward SM, Lobley AE, Nugent TC, Bryson K, Jones DT.** 2010. Protein annotation and modeling servers at university college London. Nucleic Acids Res. **38** (Web Server issue) :W563–W568. http://dx.doi.org/10.1093/nar/gkp871.
25. **Jones DT.** 1999. Protein secondary structure prediction based on position-specific scoring matrices. J. Mol. Biol. **292**:195–202.
26. **Spear PG.** 1993. Membrane fusion induced by herpes simplex virus, p 201–232. *In* Bentz J (ed), Viral fusion mechanisms. CRC Press, Boca Raton, FL.
27. **Baghian A, Huang L, Newman S, Jayachandra S, Kousoulas KG.** 1993. Truncation of the carboxy-terminal 28 amino acids of glycoprotein B specified by herpes simplex virus type 1 mutant amb1511-7 causes extensive cell fusion. J. Virol. **67**:2396–2401.
28. **Foster TP, Melancon JM, Kousoulas KG.** 2001. An alpha-helical domain within the carboxyl terminus of herpes simplex virus type 1 (HSV-1) glycoprotein B (gB) is associated with cell fusion and resistance to heparin inhibition of cell fusion. Virology **287**:18–29.
29. **Ruel N, Zago A, Spear PG.** 2006. Alanine substitution of conserved residues in the cytoplasmic tail of herpes simplex virus gB can enhance or abolish cell fusion activity and viral entry. Virology **346**:229–237.
30. **Muggeridge MI, Grantham ML, Johnson FB.** 2004. Identification of syncytial mutations in a clinical isolate of herpes simplex virus 2. Virology **328**:244–253.
31. **Diakidi-Kosta A, Michailidou G, Kontogounis G, Sivropoulou A, Arsenakis M.** 2003. A single amino acid substitution in the cytoplasmic tail of the glycoprotein B of herpes simplex virus 1 affects both syncytium formation and binding to intracellular heparan sulfate. Virus Res. **93**: 99–108.
32. **Cai WH, Gu B, Person S.** 1988. Role of glycoprotein B of herpes simplex virus type 1 in viral entry and cell fusion. J. Virol. **62**:2596–2604.
33. **Huff V, Cai W, Glorioso JC, Levine M.** 1988. The carboxy-terminal 41 amino acids of herpes simplex virus type 1 glycoprotein B are not essential for production of infectious virus particles. J. Virol. **62**:4403–4406.
34. **Gage PJ, Levine M, Glorioso JC.** 1993. Syncytium-inducing mutations localize to two discrete regions within the cytoplasmic domain of herpes simplex virus type 1 glycoprotein B. J. Virol. **67**:2191–2201.
35. **Engel JP, Boyer EP, Goodman JL.** 1993. Two novel single amino acid syncytial mutations in the carboxy terminus of glycoprotein B of herpes simplex virus type 1 confer a unique pathogenic phenotype. Virology **192**: 112–120.
36. **Bzik DJ, Fox BA, DeLuca NA, Person S.** 1984. Nucleotide sequence of a region of the herpes simplex virus type 1 gB glycoprotein gene: mutations affecting rate of virus entry and cell fusion. Virology **137**:185–190.
37. **Heineman TC, Connolly P, Hall SL, Assefa D.** 2004. Conserved cytoplasmic domain sequences mediate the ER export of VZV, HSV-1, and HCMV gB. Virology **328**:131–141.
38. **Walev I, Lingen M, Lazzaro M, Weise K, Falke D.** 1994. Cyclosporin A resistance of herpes simplex virus-induced "fusion from within" as a phenotypical marker of mutations in the Syn 3 locus of the glycoprotein B gene. Virus Genes **8**:83–86.
39. **Fan Z, Grantham ML, Smith MS, Anderson ES, Cardelli JA, Muggeridge MI.** 2002. Truncation of herpes simplex virus type 2 glycoprotein B increases its cell surface expression and activity in cell-cell fusion, but these properties are unrelated. J. Virol. **76**:9271–9283.
40. **Beitia Ortiz de Zarate I, Cantero-Aguilar L, Longo M, Berlioz-Torrent C, Rozenberg F .** 2007. Contribution of endocytic motifs in the cytoplasmic tail of herpes simplex virus type 1 glycoprotein B to virus replication and cell-cell fusion. J. Virol. **81**:13889–13903.
41. **Beitia Ortiz de Zarate I, Kaelin K, Rozenberg F .** 2004. Effects of mutations in the cytoplasmic domain of herpes simplex virus type 1 glycoprotein B on intracellular transport and infectivity. J. Virol. **78**: 1540–1551.
42. **Klupp BG, Nixdorf R, Mettenleiter TC.** 2000. Pseudorabies virus glycoprotein M inhibits membrane fusion. J. Virol. **74**:6760–6768.
43. **Tugizov S, Wang Y, Qadri I, Navarro D, Maidji E, Pereira L.** 1995. Mutated forms of human cytomegalovirus glycoprotein B are impaired in inducing syncytium formation. Virology **209**:580–591.
44. **Bold S, Ohlin M, Garten W, Radsak K.** 1996. Structural domains involved in human cytomegalovirus glycoprotein B-mediated cell-cell fusion. J. Gen. Virol. **77**:2297–2302.
45. **Pertel PE.** 2002. Human herpesvirus 8 glycoprotein B (gB), gH, and gL can mediate cell fusion. J. Virol. **76**:4390–4400.
46. **Marsh M, McMahon HT.** 1999. The structural era of endocytosis. Science **285**:215–220.
47. **Nixdorf R, Klupp BG, Karger A, Mettenleiter TC.** 2000. Effects of truncation of the carboxy terminus of pseudorabies virus glycoprotein B on infectivity. J. Virol. **74**:7137–7145.
48. **Silverman JL, Greene NG, King DS, Heldwein EE.** 2012. Membrane requirement for folding of the herpes simplex virus 1 gB cytodomain suggests a unique mechanism of fusion regulation. J. Virol. **86**:8171–8184.
49. **Royle SJ, Bobanovic LK, Murrell-Lagnado RD.** 2002. Identification of a non-canonical tyrosine-based endocytic motif in an ionotropic receptor. J. Biol. Chem. **277**:35378–35385.
50. **Royle SJ, Qureshi OS, Bobanovic LK, Evans PR, Owen DJ, Murrell-Lagnado RD.** 2005. Non-canonical YXXGPhi endocytic motifs: recognition by AP2 and preferential utilization in P2X4 receptors. J. Cell Sci. **118**:3073–3080.
51. **Park SJ, Seo MD, Lee SK, Lee BJ.** 2008. Membrane binding properties of EBV gp110 C-terminal domain; evidences for structural transition in the membrane environment. Virology **379**:181–190.
52. **Chowdary TK, Heldwein EE.** 2010. Syncytial phenotype of C-terminally truncated herpes simplex virus type 1 gB is associated with diminished membrane interactions. J. Virol. **84**:4923–4935.
53. **Ito M, Nishio M, Komada H, Ito Y, Tsurudome M.** 2000. An amino acid in the heptad repeat 1 domain is important for the haemagglutinin-neuraminidase-independent fusing activity of simian virus 5 fusion protein. J. Gen. Virol. **81**:719–727.
54. **Tong S, Li M, Vincent A, Compans RW, Fritsch E, Beier R, Klenk C, Ohuchi M, Klenk HD.** 2002. Regulation of fusion activity by the cytoplasmic domain of a paramyxovirus F protein. Virology **301**:322–333.
55. **Russell CJ, Jardetzky TS, Lamb RA.** 2001. Membrane fusion machines of paramyxoviruses: capture of intermediates of fusion. EMBO J. **20**: 4024–4034.
56. **Paterson RG, Russell CJ, Lamb RA.** 2000. Fusion protein of the paramyxovirus SV5: destabilizing and stabilizing mutants of fusion activation. Virology **270**:17–30.
57. **Waning DL, Russell CJ, Jardetzky TS, Lamb RA.** 2004. Activation of a paramyxovirus fusion protein is modulated by inside-out signaling from the cytoplasmic tail. Proc. Natl. Acad. Sci. U. S. A. **101**:9217–9222.
58. **Silva AL, Omerovic J, Jardetzky TS, Longnecker R.** 2004. Mutational analyses of Epstein-Barr virus glycoprotein 42 reveal functional domains not involved in receptor binding but required for membrane fusion. J. Virol. **78**:5946–5956.
59. **Omerovic J, Lev L, Longnecker R.** 2005. The amino terminus of Epstein-Barr virus glycoprotein gH is important for fusion with epithelial and B cells. J. Virol. **79**:12408–12415.
60. **Wu L, Borza CM, Hutt-Fletcher LM.** 2005. Mutations of Epstein-Barr virus gH that are differentially able to support fusion with B cells or epithelial cells. J. Virol. **79**:10923–10930.